Proceedings of the ASME 2019 38th International Conference on Ocean, Offshore and Arctic Engineering
OMAE2019
June 9-14, 2019, Glasgow, Scotland

OMAE2019-95970

FORCED VIBRATION TESTS FOR IN-LINE VIV TO ASSESS PARTIALLY STRAKE-COVERED PIPELINE SPANS

Jie Wu[1], Decao Yin, Elizabeth Passano, Halvor Lie
SINTEF Ocean
Trondheim, Norway

Ralf Peek
Peek Solutions
St. Andreu de Llavaneres, Spain

Octavio E. Sequeiros, Sze Yu Ang
Shell Global Solutions International B.V.
Rijswijk, The Netherlands

Chiara Bernardo, Meliza Atienza
Shell Philippines Exploration B.V.
Manila, Philippines

ABSTRACT

A series of experiments is performed in which a strake-covered rigid cylinder undergoes harmonic purely in-line motion while subject to a uniform "flow" created by towing the test rig along SINTEF Ocean's towing tank. These tests are performed for a range of frequencies and amplitudes of the harmonic motion, to generate added-mass and excitation functions are derived from the in-phase and 90° out-of-phase components of the hydrodynamic force on the pipe, respectively.

Using these excitation- and added-mass functions in VIVANA together with those from experiments on bare pipe by Aronsen (2007), the in-line VIV response of partially strake-covered pipeline spans is calculated. It is found that as little as 10% strake coverage at the optimal location effectively suppresses pure in-line VIV.

Further advantages of strakes rather than intermediate supports to suppress in-line VIV include: strakes are not affected by the scour which can lower an intermediate support (in addition to creating the span in the first place). Further they do not prevent self-lowering of the pipeline or act as a point of concentration of VIV damage as the spans to each side of the intermediate support grow again.

Keywords: VIV, pure in-line response, partial strake coverage, free-spanning pipeline, VIVANA, SIVANA.

NOMENCLATURE

A	Displacement amplitude (m)
CF	Cross-flow
C_e	IL excitation (lift) coefficient
C_a	IL added mass coefficient
C_d	Drag coefficient
D	Outer diameter of the bare pipe (m)
$e_{strakes}$	Offset distance of strake from the midpoint of the free span divided by the span length
F	Measured hydrodynamic forces on the test cylinder (N)
f_n	Natural frequency in still water (Hz)
f_{osc}	Oscillation frequency (Hz)
$\hat{f}$	Non-dimensional oscillation frequency, $\hat{f} = f_{osc}D/U$
H	Height of a strake (m)
IL	In-line
k	Roughness (m)
k/D	Roughness ratio
K	Soil stiffness (N/m^2)
L	Length of the test cylinder (m)
L_{span}	Free span length of single span pipeline (m)
$L_{strakes}$	Length of the strakes (m)
m	Mass of the test cylinder (kg)
P	Pitch of a strake (m)
R_e	Reynolds number
T	Oscillation period (sec)
x_0	IL displacement amplitude (m)
U	Current velocity (m/s)
U_r	Reduced velocity based on the natural frequency in

[1] Contact author: jie.wu@sintef.no

still water, $U_r = U/f_n D$

V_r Reduced velocity based on the oscillation frequency, $V_r = U/f_{osc} D$

VIV Vortex-induced vibrations

$\lambda_{strakes}$ Strake coverage ratio $\lambda_{strakes} = L_{strakes}/L_{span} \times 100\%$

INTRODUCTION

Fatigue damage from Vortex-induced vibrations (VIV) can threaten the integrity of pipelines at free spans. Such spans arise not only due to pipelay on an uneven seabed, but also due to scour. Traditionally intermediate supports (such as grout bags) are introduced if a span becomes too long. However, intermediate supports have a number of disadvantages, especially for scour-induced spanning: they do not allow the pipeline to self-lower into the scour trench it creates; the grout bags or other intermediate supports may themselves be undermined by scour, thus being lowered and rendered ineffective; finally, the scouring will typically continue with the intermediate support in place creating two spans that can reach critical length with the intermediate support becoming a point of concentration of fatigue damage.

On the other hand, strakes, such as those shown in Figure 2, have none of the above disadvantages. Thus, they provide a more durable and reliable solution, provided that they effectively suppress VIV.

Although cross-flow (CF) VIV can have higher amplitudes than in-line (IL) VIV, IL VIV develops at much lower current velocities. As a result, often most of the fatigue damage (as determined based on DNV RP F-105 [13]) comes from in-line VIV. It is shown here based on combination of forced in-line vibration tests on a straked pipe and analysis that as little as 14% strake coverage is sufficient to effectively suppress such in-line VIV.

Whereas the use of strakes to suppress cross-flow VIV has been the subject of a number of investigations [19], [21], [22], [23], no experimental data were available to quantify the effect of partial strake coverage on in-line VIV. Yet for pure in-line VIV frequency domain (FD) methods based on empirically established excitation and added-mass functions are particularly well suited, because the response is purely horizontal and does suffer from the complications arising from coupling between vertical and horizontal response and excitation [15].

VIV of free spanning pipeline has been extensively studied in the recent years [16], [18]. Design guideline DNV RP F-105 [13] has been developed based on these earlier research [1]. However, the current guideline cannot handle pipeline with partial strake coverage.

Strakes are commonly used as VIV suppression devices. The suppression efficiency depends on strake's height and pitch over diameter ratios (H/D, P/D) [19]. Experiments with flexible cylinders showed that significant amount of strake coverage (>82% in some tests) may be needed in order to fully suppress cross-flow (CF) VIV responses [21], [22], [23]. There are no available test data to determine the strake coverage for suppressing pure in-line (IL) responses with the required strake profile (P/D=17.5, H/D=0.25).

Frequency domain (FD) empirical VIV prediction tools, such as VIVANA-FD [4], are often used by the industry to predict VIV responses of slender marine structures. It has been applied to free spanning pipelines [3], [5]. A simplified tool, SIVANA, is developed by Peek [12] based on the similar methodology. A new time domain (TD) tool has been implemented in VIVANA-TD, which has shown its potential to describe VIV responses subjected to non-stationary flow and non-linear boundary conditions [8].

These tools rely on empirical hydrodynamic coefficient data generalized from model tests [6], [7]. CF hydrodynamic data for strakes have been reported[17], [20], [24]. However, there is lack of hydrodynamic coefficient data for strakes (P/D=17.5, H/D=0.25) under pure IL response conditions.

The present work focus on prediction of pure IL responses of a free spanning pipeline with partial strake coverage [9], [10], [11]. It consists of two parts, i.e., experimental work and numerical case study. Firstly, forced motion test with strake on a rigid cylinder was carried out in the towing tank in SINTEF Ocean in 2017. Additional tests were also performed with a rough bare cylinder to investigate the sensitivity on VIV responses due to the roughness.

Then, a numerical case study of a typical free spanning pipeline using VIVANA-FD and SIVANA with hydrodynamic coefficients obtained from the experiment was carried out. VIV response of a typical pipeline was simulated in order to determine the sufficient strake coverage level that can fully suppress pure IL VIV responses. Sensitivity on the strake placement was also investigated, considering the span length variation due to the effect of mobile sand. The pure IL response prediction of the bare pipe is discussed in the accompany paper [15].

MODEL FORCED-VIBRATION TEST

Test Setup

The model test was performed in SINTEF Ocean's (former MARINTEK) towing tank, which have a total length of 260 m and a breadth of 10.5 m. The water depth is 5.6 m/10.0 m in different sections of the tank. Rigid-cylinder, IL forced-vibrations VIV tests were performed by imposing an in-line harmonic motion on the test pipe, and measuring the resulting hydrodynamic forces. A steady constant current velocity is simulated by "towing" the test rig. The assembly shown in Figure 1 is supported by a gantry system on rails that spans the test tank and moves at constant velocity to simulate the steady current. The harmonic motion is imposed by the Hexapod

(yellow actuators in Figure 1 that control all 6 degrees of freedom of the rigid plate below). Below that is the test rig supporting the fully straked test cylinder, as shown in Figure 1.

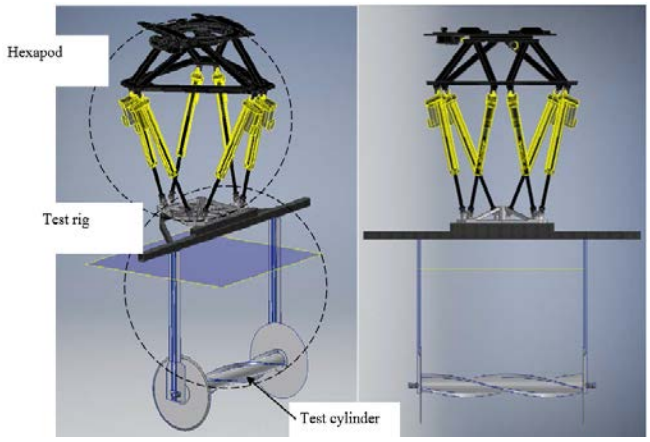

Figure 1Test setup. Not all of the structural details are included in this illustration.

Test Models

Two aluminum cylinders were manufactured for the tests. A strip was welded along one of the cylinders to model the a typical three-start strake. A rough cylinder is modelled by wrapping sandpaper around the bare smooth cylinder at the end of the test. Therefore, three cylinder models were tested, see Figure 2 and Figure 3. The property of the cylinders is summarized in

Table 1. The roughness of a new aluminum pipe is about 1×10^{-6}-2×10^{-6} m [25]. Standard sand paper P24 was glued on the bare smooth cylinder to simulate the roughness of the pipeline with concrete coating. There is no visible deterioration of the sandpaper during the test. The corresponding roughness is 7.6×10^{-4} m [26]. The ends of the models are made watertight.

Table 1 Properties of the test models

Cylinder	Dry Mass (kg)	Roughness ratio, k/D
Bare smooth	20.3	$0.5 - 1.0\times10^{-5}$
Straked	22.6	N/A
Bare rough	22.8	3.6×10^{-3}

Figure 2 Test models

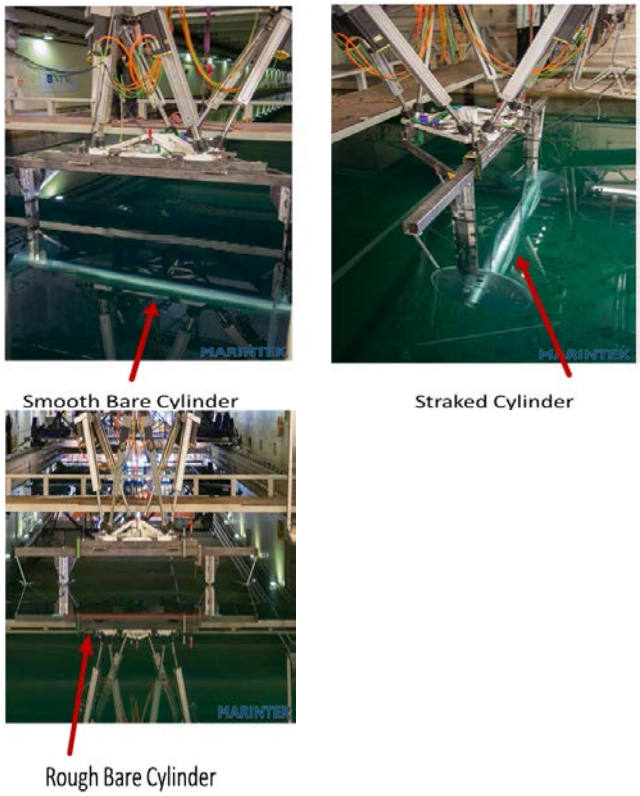

Figure 3 Tested configurations

The diameter of the test cylinders is D=0.2 m and the length is L=2.333 m. The length over diameter ratio (L/D) is 11.67. The pitch of the strake is 17.5D, or 3.5 m. This length of the test cylinder is 2/3 of one complete pitch of the strake. (The strakes pipe is periodic with a period of one third of the pitch, so that the test specimen is two periods long.) Due to this symmetry, the test cylinder is assumed to be independent of the orientation of the test cylinder. The height of the strake is 0.25D, or 0.05 m. The definition of the pitch and height can be found in Figure 3-5.

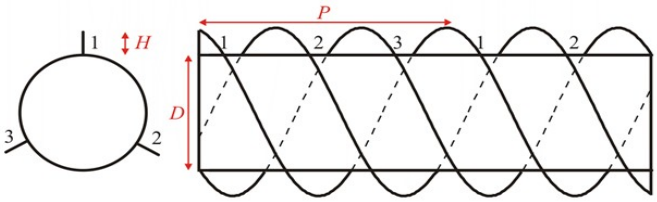

Figure 4 Definition of pitch and height of a three-start strake.

Instrumentation

Two 2-component force transducers are installed at the end of the test cylinder. Two 3-component accelerometers were positioned close to the end plate to monitor the vibrations of the test rig. Additional accelerometers were placed on the Hexapod and carriage. An optical tracking system (OQUS) system was used to measure the movement of the test rig, in addition to the direct output data from Hexapod. Three light balls are placed on the Hexapod and their movements are measured by OQUS. The sampling frequency of the force transducer and the

accelerometer is 200 Hz. The sampling frequency of the OQUS system is 25 Hz. The Hexapod signal was re-sampled at 200 Hz.

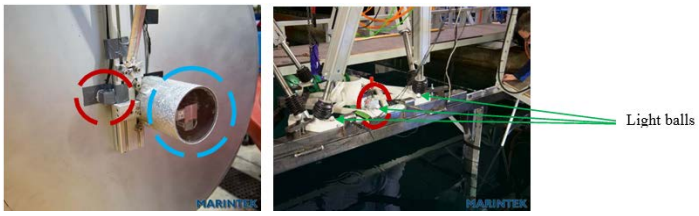

Figure 5 Instrumentations. Accelerometers are marked in red circles, end force transduced is located in the blue circle and the light balls for OQUS system is marked by green arrows.

Test Results

1) Stationary test

The drag coefficients of a circular cylinder can be found in various literature. The drag coefficients ($C_d = \bar{F}_{IL}/\frac{1}{2}\rho DLU^2$) of the smooth and rough cylinder are shown in Figure 6. They compare very well with those in DNV RP-C025 [14]. The drag coefficient of the smooth bare cylinder (k/D=5×10^{-6} - 1×10^{-5}) is about 1.2 in the range of Re=2.4×10^4 – 1.75×10^5. The drag coefficient of the rough cylinder shows a clear drag crisis around Re=5.3×10^4 as expected. The lowest drag coefficient is 0.71 and the value increases to about 1.0 outside of the crisis (Re>1.0×10^5). Aronsen [6] reported drag coefficient about 1.3 for the bare cylinder with similar surface roughness in Re=1.0 – 2.4×10^4.

The drag coefficient of a straked cylinder is not influenced by the Reynolds number effect compared to a bare cylinder as shown in Figure 6. The strake used in present test has a pitch of 17.5D and height of 0.25D. The AIMS strake [24] has slightly higher pitch/height than the tested strakes and a slightly higher drag coefficient of 1.4 from present tests are therefore expected.

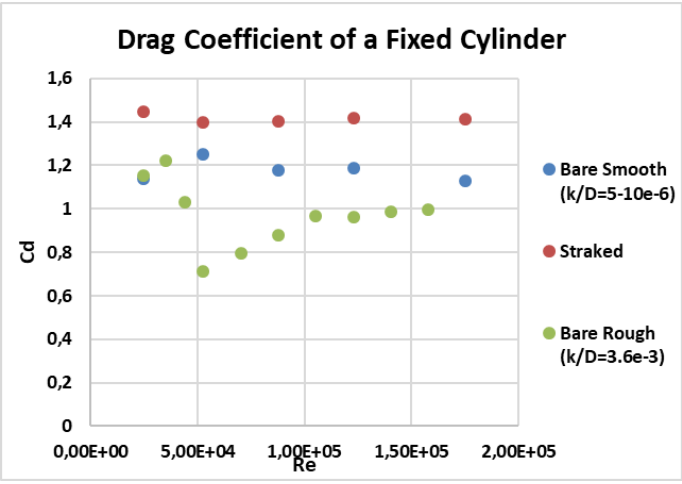

Figure 6 Drag coefficient of the stationary cylinder test

2) Forced Motion Test with a Bare Cylinder

The main purpose of these tests on bare cylinders is to check that the test rig is working as intended by comparing results with existing ones. Excitation and added mass coefficients are defined as:

$$C_e = 2\lim_{T\to\infty}\frac{\int_t^{t+T} F_{IL}\dot{y}dt}{T}\Big/\left(\frac{1}{2}\rho LDU^2\omega x_0\right) \qquad \textbf{Equation 1}$$

$$C_a = 2\lim_{T\to\infty}\frac{\int_t^{t+T} F_{IL}\ddot{y}dt}{T}\Big/\left(\rho\pi\frac{D^2}{8}L(\omega^2 x_0)^2\right) \qquad \textbf{Equation 2}$$

Where, F_{IL} is the IL hydrodynamic force, m is the mass of the cylinder. x is the IL motion with amplitude of x_0 and angular frequency $\omega = \frac{2\pi}{T}$. Dots represent time derivatives of the variable. Trapezoidal numerical integration is applied.

The coefficients corresponding to the bare smooth cylinder are compared with Aronsen's test results [6] in Figure 7 and Figure 8, respectively. In these figures, the present test data are shown as blue points with force coefficients value in red. The general trend is consistent with Aronsen's results. The Reynolds number of the present test (5.3×10^4) is 2.25 times of that in Aronsen's test. A lower towing speed (U=0.14 m/s) would need to be used in order to achieve the same Reynolds number. However, the hydrodynamic forces at such low speed may be too small compared to the disturbance due to the carriage/rig vibrations. Higher towing speed than 0.3 m/s is also less favored in order to be away from the natural frequency of the test rig. Therefore, most of the present tests were carried out at 0.3 m/s. Though there should be no significant Reynold number effect for a smooth bare cylinder in this flow regime, small differences in force coefficient values can be expected.

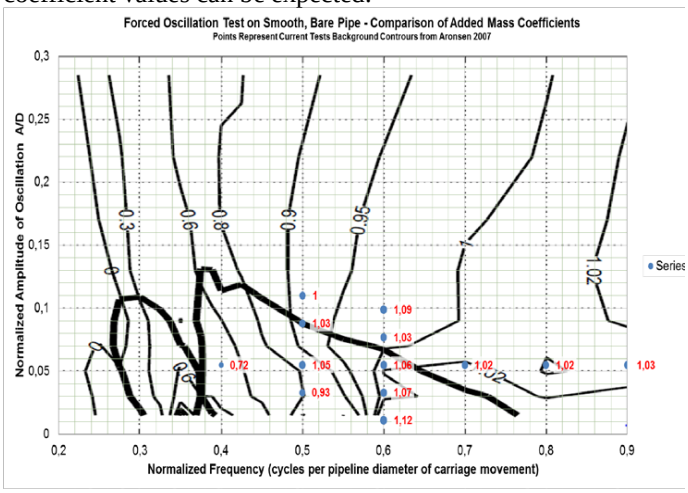

Figure 7 IL added mass coefficient for the smooth bare cylinder (U=0.3m/s, Re=5.3×10^4)

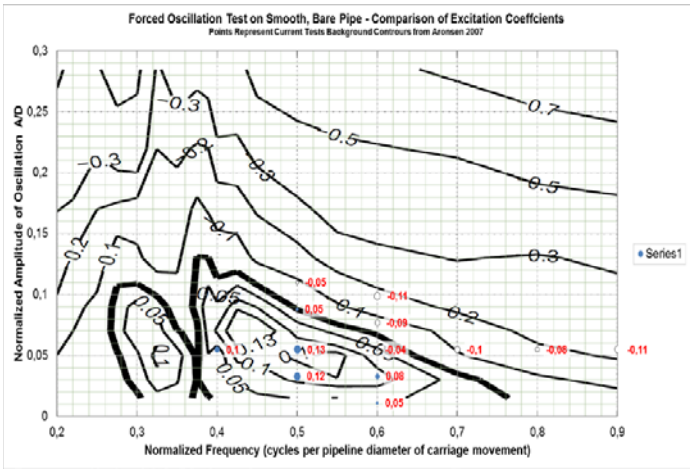

Figure 8 IL excitation (lift) coefficient for the smooth bare cylinder (U=0.3m/s, Re=5.3×10^4)

It is concluded based on the bare smooth cylinder test results that the test setup and instrumentation are reliable.

Forced Motion Test with a Straked Cylinder

These tests yielded the needed results for which no data were available. The excitation (lift) coefficients are presented against the amplitude ratio (A/D) for different reduced velocities ($V_r = U/f_{osc}D$) in Figure 9. These coefficients are also presented in a contour plot in Figure 10. The horizontal axis is the non-dimensional frequency, which is inverse of the reduced velocity V_r. The results show that strakes provide damping forces as indicated by the negative excitation values. This means that the strake will suppress VIV amplitude by dissipating energy.

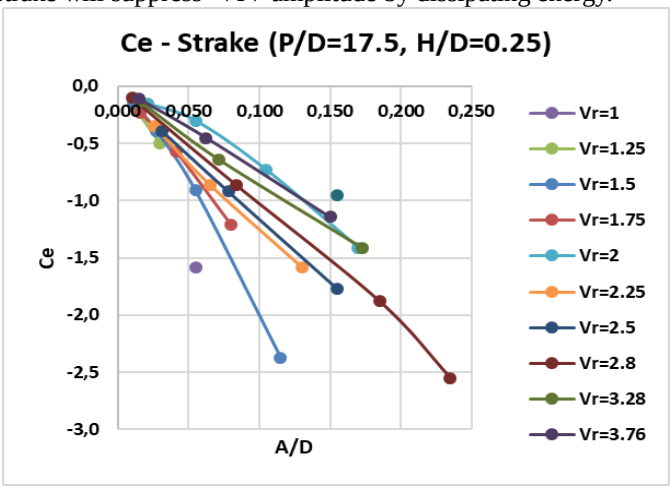

Figure 9 IL excitation (lift) coefficient for the straked cylinder (U=0.3m/s, Re=5.3×10^4)

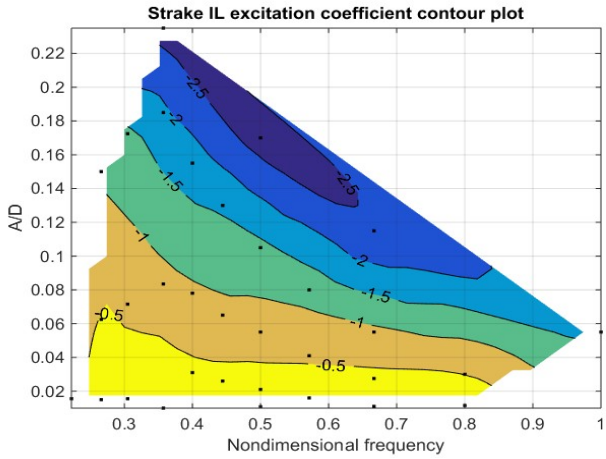

Figure 10 Contour plot the IL excitation (lift) coefficient for the straked cylinder (U=0.3m/s, Re=5.3×10^4). The black dots are the actual data points.

The added mass coefficients are presented in Figure 11. The values are between 1.3 to 1.7.

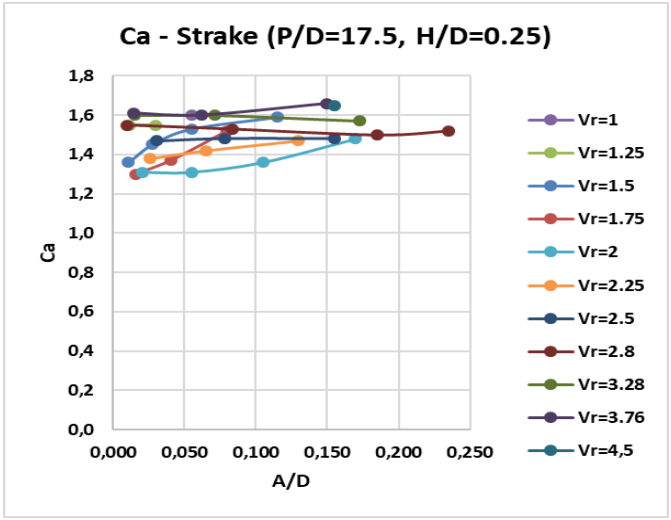

Figure 11 IL added mass coefficient for the straked cylinder (U=0.3m/s, Re=5.3×10^4)

The drag coefficients for straked cylinder subjected to pure IL motions are presented in Figure 12. They are in general larger than the drag coefficients found in stationary tests.

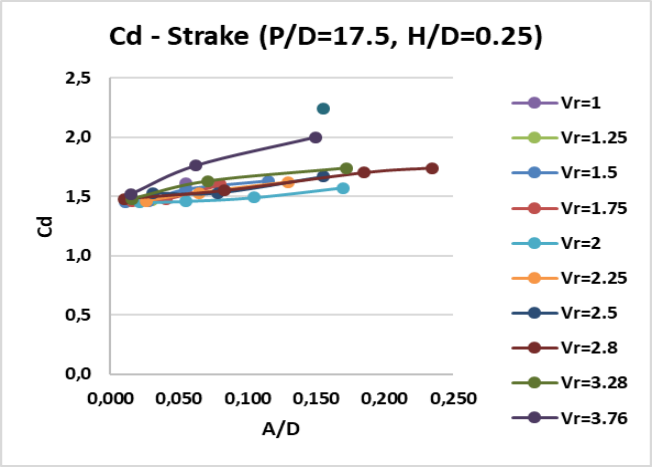

Figure 12 Drag coefficient from the pure IL forced motion tests with straked cylinder (U=0.3m/s, Re=5.3×10^4)

3) Forced Motion Test with a Bare Rough Cylinder

Bare rough cylinder tests were carried out at 0.3 m/s and the excitation coefficient are presented in Figure 19 in Appendix A. The excitation coefficients are very similar to those of a bare smooth cylinder from Aronsen's test, especially in the first instability region from non-dimensional frequency 0.38 to 0.76. The A/D envelope corresponds to zero excitation coefficient seems to be larger for a very rough cylinder. The A/D where Ce equals to zero is about 0.09 at non-dimensional frequency 0.6 compared to 0.07 found in Aronsen's test. There are limited data points from non-dimensional frequency 0.27 to 0.38. Therefore, it is difficult to evaluate the differences compared to a smooth cylinder in this region.

Several sensitivity tests at three different towing speeds, 0.2 m/s, 0.3 m/s and 0.5 m/s were also conducted.

NUMERICAL STUDY OF PIPELINE WITH PARTIAL STRAKE COVERAGE

Overview

VIV responses of a typical pipeline using VIVANA-FD [4] for different span and strake configurations are evaluated by a numerical case study. This includes bare/straked, single span/multi-span cases. The performance of strakes with an offset from the mid-span was also evaluated, considering the effect of mobile sand.

In essence, VIVANA-FD solves the frequency-domain problem including the nonlinearity arising from the empirically-determined added mass and excitation functions. This yields response frequencies and complex dynamic response modes that can including point-to-point changes in phase whereby propagating wave effects are captured. Such propagating wave effects are important for risers in that it transports energy from excitation zones to damped zones. However, pipeline spans are much shorter than the typical riser, which enables a simplified approach referred to here by "SIVANA". This a Rayleigh-Ritz approximation to the VIVANA-FD approach, in which the assumed mode-shape of the response corresponds to the undamped free vibration mode of the bare pipe. The amplitude and frequency of the SIVANA response is determined by the Rayleigh-Ritz approximation. It does not involve point-to-point changes in phase of the response. A comparison between VIVANA-FD and SIVANA predictions is presented in the end.

An overview of the analyzed cases is presented in Table 2. The structural properties of the pipeline are summarized in Table 4 in Appendix B. The sketches of each configurations are presented in Figure 20 in Appendix C. Except for Configurations 4, 5 and 9, the interval between adjacent two springs on the shoulders is 2 m, which is also the element length at the shoulders. A refined structural model was applied for the Configurations 4, 5 and 9, the element length was also shortened to 0.5 m for the pipe on the shoulders. The distributed soil springs of stiffness per unit length K are approximated by discrete springs at the nodal points, for which the stiffness is K times a tributary length. This tributary length is taken to be the element length for all nodes within the soil-supported zone. However, at the shoulder of the span (i.e. at the transition from the soil-supported to the free-spannning condition), the tributary length is taken to be half an element length.

Table 2 Overview of the free span pipeline configurations for various span lengths (L_{span}), strake coverage ($\lambda_{strakes}$) and eccentricity of strakes from mid-point of the free span ($e_{strakes}$) and VIVANA-FD analysis.

				VIVANA Analysis	
Configuration	L_{span} (m)	$\lambda_{strakes}$ (%)	$e_{strakes}$ (%)	IL	CF
1	40	0	-	√	
2		10	0	√	
3		10	25	√	
4[3)]	54	0	-		√
5[3)]		10	0	√	√
6		10	10	√	
7		10	25	√	
8		2×10[1)]	25	√	
9[3)]		25	25	√	
10	Multi	0	-	√	
11		10[2)]	0	√	

1) Two sections of strakes with the length of $10\%L_{span}$ used, with $e_{strakes} = 25\%$
2) Strakes cover the 1st, 2nd and 6th span, all strake sections have the standard manufactured length 3.35 m.
3) Refined structural model at the shoulders, with element length=0.5 m.

Semi-empirical VIV Prediction Program VIVANA-FD

The VIVANA-FD program is a semi-empirical frequency domain program based on the finite element method. The program was developed by SINTEF Ocean and the Norwegian University of Science and Technology (NTNU) to predict VIV responses. The fluid-structure interaction in VIVANA is described using added mass, excitation and damping coefficients. In addition to pure CF response analysis, the program can also predict pure IL response, which occurs at low current levels, before the onset of CF VIV response.

All analyses in the present study were carried out using VIVANA 4.9.0, a development version which can import user-defined IL hydrodynamic force coefficients compared to the earlier version of the program. The hydrodynamic input data used in present study is summarized in **Table 3**.

Table 3 Hydrodyamic input data

Force coefficient	Ce	Ca
Bare pipe*	Default [4]	Default [4]
Straked pipe	Direct use of present test data (Figure 9)	1.7 based on present test data (Figure 11)

*: Bare cylinder data is generalized from Aronsen's test [6]

VIVANA-FD Case Study Results

1) **Single span $L_{span} = 40\ m$**

VIV at 7 current speeds were evaluated, corresponding to the reduced velocity $U_r = U/f_n D$ from 1 to 2.5. The displacement and stress amplitude of the bare pipe case (configuration 1, including stiffness-proportional damping and soil damping) are presented in Figure 13.

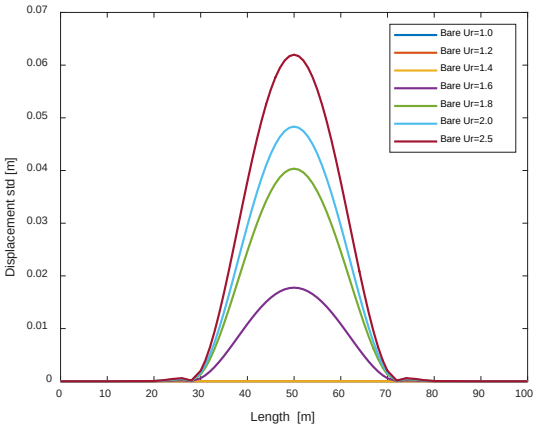

Figure 13 Predicted displacement amplitude along the pipeline of Configuration 1. (Bare pipe)

The maximum A/D along the free span for different cases are presented against Ur and the DNV RP-F105 response curve in Figure 14. The VIVANA prediction of the undamped case compares well with the DNV response curve. The structural damping and soil damping values are set to be zero for the undamped cases. Otherwise, the structural damping ratio and the soil damping ratio are set to be 1.5% and 10% of the critical damping respectively.

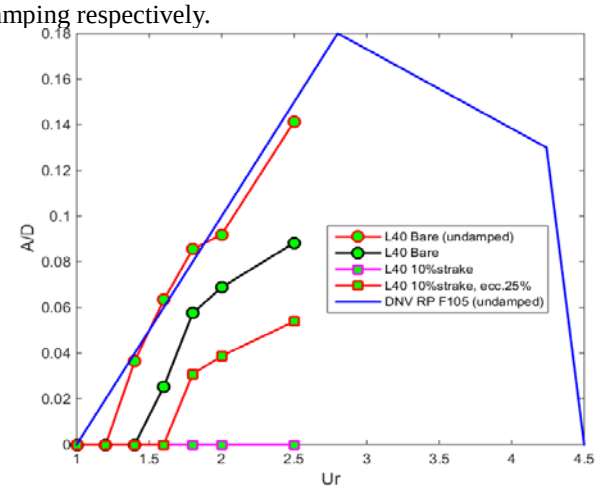

Figure 14 Maximum A/D vs. U_r of all configurations with $L_{span} = 40$, comparison against DNV RP-F105 response curve.

2) **Single span $L_{span} = 54\ m$**

The maximum A/D along the free span for different cases are presented against Ur and the DNV RP-F105 response curve in Figure 15. Pure IL VIV is completely suppressed except for when the strakes are placed with an offset of 25% of free span length from the mid-point.

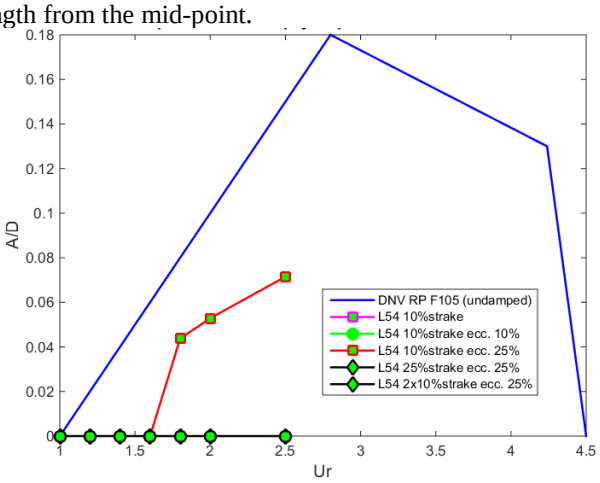

Figure 15 Maximum A/D vs. U_r of all configurations with $L_{span} = 54$, comparison against DNV-RP-F105 response curve.

3) **Multi-span**

There are 6 spans with the longest span length of 39 m, refer to Configuration 11 in Figure 20 in the appendix. Strakes cover

the 1st, 2nd and 6th span, all strake sections have the standard manufactured length 3.35 m. This gives approximately 10% of strake coverage for the longest span.

The displacement amplitude of the bare pipe case (configuration 10, including stiffness-proportional damping and soil damping) are presented in Figure 16 and Figure 17. Pure IL VIV is completely suppressed with 10% of strake coverage in the mid-span.

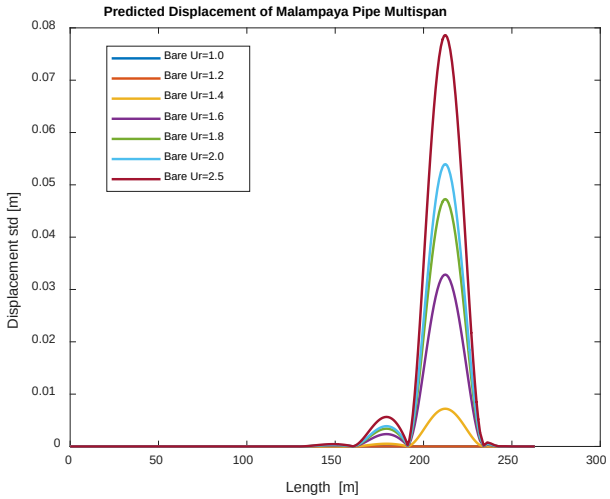

Figure 16 Predicted displacement along the pipeline of Configuration 10 (Bare pipe).

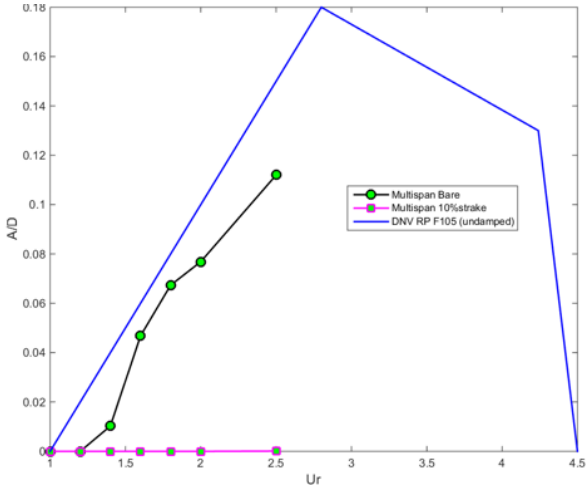

Figure 17 Maximum A/D vs. U_r of multi-span configurations, comparison against DNV-RP-F105 response curve.

Comparison of VIVANA-FD and SIVANA Prediction

An example comparing VIVANA-FD results with SIVANA results is included in Figure 18 for 10% strake coverage offset from midspan by 25% of the span length. The good agreement confirms that travelling wave effects or other changes in mode shape are not important in this case. Similarly, good agreement was obtained for the fully bare pipe. It is further estiamted by SIVANA that 14% of strake coverage at the mid-span can fully suppress pure IL VIV without any soil and structural damping.

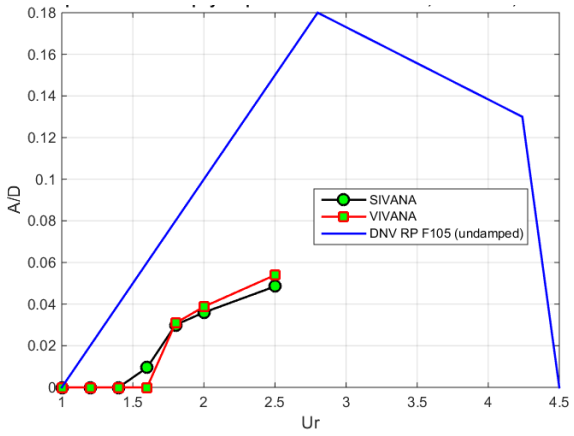

Figure 18 Comparison of in-line VIV response for 10% strake with 25% of eccentricity calculated with VIVANA and with the simplified, SIVANA approach.

CONCLUSIONS

In present work, model test and numerical study have been performed to provide valuable hydrodynamic data for strakes (three-start with P/D=17.5, H/D=0.25) and determine the required strake coverage level for suppressing pure IL VIV responses of a free spanning pipeline. VIVANA-FD and SIVANA tools have been used in the numerical study.

In addition to the structural and soil damping, strakes provide significantly higher damping contribution and reduce VIV responses. The numerical study shows that 10% of strake coverage in mid-span can effectively suppress pure IL VIV responses. This is significantly lower than the required coverage level for suppressing CF responses based on experiences from earlier high mode VIV model tests. Suppression efficiency decreases with increasing offset of the strake from the mid-span. Note that this conclusion is based on a typical pipeline property with specified soil conditions. A different strake coverage level might be expected for a different condition. However, the methodology, tools and hydrodynamic data presented in this work is applicable to VIV assessment of free spanning pipelines in general.

ACKNOWLEDGEMENTS

The authors are grateful to Shell Global Solutions International B.V. and Shell Philippines Exploration B.V. for their financial support and permission to publish this work.

REFERENCES

[1] Nielsen, F. G., Søreide, T. H., and Kvarme, S. O., 2002. "VIV Response of Long Free Spanning Pipelines". In ASME 2002 21st International Conference on Offshore Mechanics and Arctic Engineering, no. OMAE2002- 28075.

[2] Larsen, C. M., Koushan, K., and Passano, E., 2002. "Frequency and Time Domain Analysis of Vortex Induced Vibrations for Free Span Pipelines". In ASME 2002 21st International Conference on Ocean, Offshore and Arctic Engineering, no. OMAE2002-28064.

[3] Larsen, C. M., Passano, E., Baarholm, G. S., and Koushan, K., 2004. "Non-linear Time Domain Analysis of Vortex Induced Vibrations for Free Spanning Pipelines". In ASME 2004 23rd International Conference on Ocean, Offshore and Arctic Engineering, no. OMAE2004-51404.

[4] SINTEF Ocean: VIVANA 4.12.2 Theory Manual, 2017.

[5] Passano, E., Larsen, C. M., and Wu, J., 2010. "VIV of Free Spanning Pipelines: Comparison of Response from Semi-Empirical Code to Model Tests". In ASME 2010 29th International Conference on Ocean, Offshore and Arctic Engineering, no. OMAE2010-20330.

[6] Aronsen, K. H., 2007. "An Experimental Investigation of In-line and Combined In-line and Cross-flow Vortex Induced Vibrations". PhD thesis, Norwegian University of Science and Technology, Norway.

[7] Aglen, I. M., 2013. "VIV in Free Spanning Pipelines". PhD thesis, Norwegian University of Science and Technology, Trondheim, Norway.

[8] Ulveseter, J. V., Sævik, S., and Larsen, C. M., 2016. "Vortex Induced Vibrations of Pipelines with Non-Linear Seabed Contact Properties". In ASME 2016 35th International Conference on Ocean, Offshore and Arctic Engineering, no. OMAE2016-54424.

[9] Yin, D., and Wu, J., 2017. Estimation of In Line VIV for free spanning pipelines partially covered by strakes. MARINTEK Report MT2016 F-122, SINTEF Ocean, Trondheim, Norway.

[10] Wu, J., 2017. Estimation of In-Line VIV for free spanning pipelines partially covered by strakes – Model Test. MARINTEK Report MT2016 F-146, MARINTEK, Trondheim, Norway.

[11] Wu, J., and Yin, D., 2017. Estimation of In-line VIV for free spanning pipelines partially covered by strakes Phase 2 – Numerical analysis. SINTEF Report OC2017-F028, SINTEF Ocean, Trondheim, Nor- way.

[12] Peek, R., 2017. Methodology for Fatigue Assessment for Spans Partially Covered Strakes for In-Line VIV. Tech. rep., Peek Solutions.

[13] DNVGL, 2017. DNV-RP-F105 Free spanning pipelines.

[14] DNVGL, 2010. DNV-RP-C205: Environmental conditions and environmental loads, October 2010.

[15] Yin, D., Wu, J., Passano, E., Lie, H., Peek, R., Sequeiros, O. E., Ang, S.-Y., Bernardo, C. A. and Atienza, M., 2019. "In-line VIV Based on Forced Vibration Tests". In ASME 2019 38th International Conference on Ocean, Offshore and Arctic Engineering, no. OMAE2019-95972.

[16] Huse, E., 2001. Ormen Lange 3D Model Tests. MARINTEK Report MT51-F01.040, MARINTEK, Trondheim, Norway.

[17] Huse, E. and Sæther, L.K., "VIV excitation and damping of straked risers", 20th International Conference on Ocean, Offshore and Arctic Engineering, 2001.

[18] Mo, K., and Solaas, F., 2002. Ormen Lange 3D Phase II Modal Analysis. techreport, MARINTEK, Trondheim, Norway.

[19] Baarholm, R., and Lie, H., "Systematic parametric investigation of the efficiency of helical strakes", DOT2005, Vitoria, Brazil, November 2005.

[20] Ding, Z.J., Balasubramanian, S., Lokken, R.T. and Yung, T-W., "Lift and Damping Characteristics of Bare and Straked Cylinders at Riser Scale Reynolds Numbers". Offshore Technology Conference Proceedings 2004, OTC16341.

[21] Lie H, Braaten H, Jhingran V, Sequeiros OE, Vandiver K. Comprehensive Riser VIV Model Tests in Uniform and Sheared Flow. ASME. International Conference on Offshore Mechanics and Arctic Engineering, Volume 5: Ocean Engineering; CFD and VIV ():923-930. doi:10.1115/OMAE2012-84055.

[22] Tognarelli, M. A., Slocum, S., Frank, W., and Campbell, R., 2004, "VIV Response of a Long Flexible Cylinder in Uniform and Linearly Sheared Currents," Offshore Technology Conference, Paper No. OTC16338.

[23] Trim, A. D., Braaten, H., Lie, H., and Tognarelli, M. A., 2005, "Experimental Investigation of Vortex-Induced Vibration of Long Marine Risers," J. Fluid Struct., 21(3), pp. 335–361.

[24] Spence, D. et al, Enabling enhancements of riser VIV design techniques through detailed interpretation of test results for VIV suppression devices. OTC 18973.

[25] http://www.engineeringtoolbox.com/surface-roughness-ventilation-ducts-d_209.html

[26] https://en.wikipedia.org/wiki/Sandpaper

Appendix A: Excitation coefficient of a rough cylinder

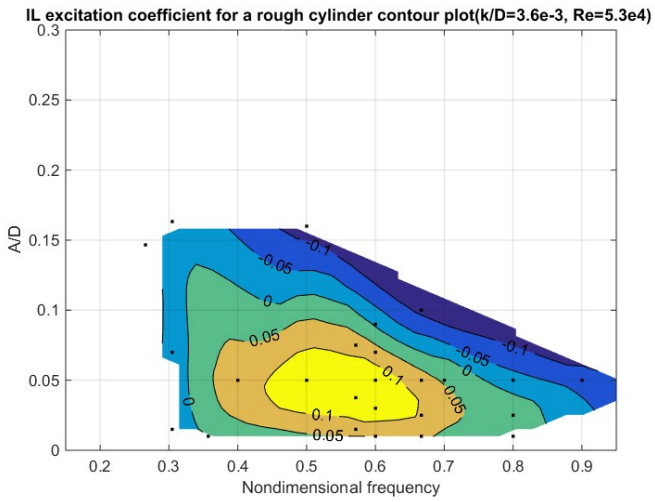

Figure 19 Pure IL excitation coefficient for bare rough cylinder forced motion tests (U=0.3m/s, k/D=3.6×10^{-3}, Re=5.3×10^{4}). The black dots in the figure are the actual data points.

Appendix B: Structural Properties of the Pipe in Case Study

Table 4 Structural properties of the pipe

Pipe inner diameter	0.576	m
Concrete outer diameter	0.690	m
Hydrodynamic diameter, D	0.702	m
Free span length, L	40.000	m
L/D	56.980	
anti-corrosion mass	682	kg
concrete mass	7351	kg
Steel pipe mass	10001	kg
Elastic modulus of steel, E2	2.07E+11	Pa
Elastic modulus of concrete, E1	30688.438	Mpa
Second moments of area, steel, I2	1.40E-03	m^4
Second moments of area, concrete, I1	4.33E-03	m^4
Steel pipe bending stiffness, EI	2.90E+08	Nm^2
Concrete bending stiffness, EIconc	1.33E+08	Nm^2
Medium sand:		
Cv	1.45E+07	$N/m^{5/2}$
Cl	1.25E+07	$N/m^{5/2}$
Poisson's ratio, v	0.500	
Density of seawater, rho	1025.000	kg/m^3
Density of the pipe, rho_s	3559.920	kg/m^3
Mass ratio, rho_s/rho	1.223	

Appendix C: Configurations of the Case Study

(1) Configuration 1: $L_{span} = 40$, $\lambda_{strakes} = 0\%$, $e_{strakes} = 0\%$

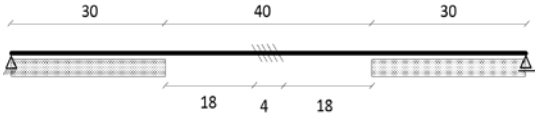

(2) Configuration 2: $L_{span} = 40$, $\lambda_{strakes} = 10\%$, $e_{strakes} = 0\%$

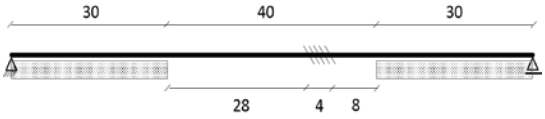

(3) Configuration 3: $L_{span} = 40$, $\lambda_{strakes} = 10\%$, $e_{strakes} = 25\%$

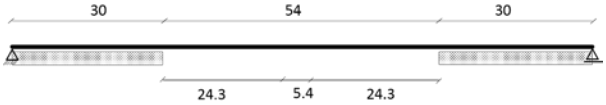

(4) Configuration 4: $L_{span} = 54$, $\lambda_{strakes} = 0\%$, $e_{strakes} = 0\%$

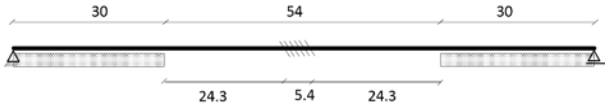

(5) Configuration 5: $L_{span} = 54$, $\lambda_{strakes} = 10\%$, $e_{strakes} = 0\%$

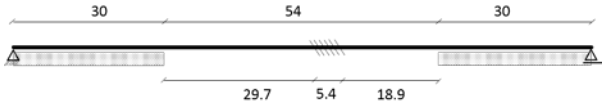

(6) Configuration 6: $L_{span} = 54$, $\lambda_{strakes} = 10\%$, $e_{strakes} = 10\%$

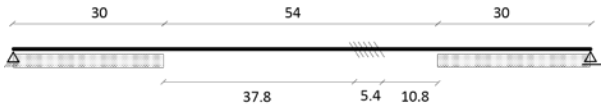

(7) Configuration 7: $L_{span} = 54$, $\lambda_{strakes} = 10\%$, $e_{strakes} = 25\%$

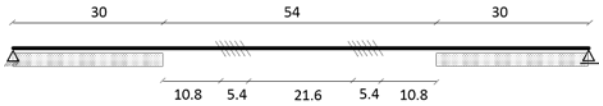

(8) Configuration 7: $L_{span} = 54$, $\lambda_{strakes} = 10\%$, $e_{strakes} = 25\%$, 2 strake sections

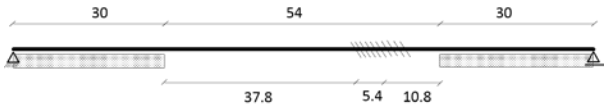

(9) Configuration 9: $L_{span} = 54$, $\lambda_{strakes} = 25\%$, $e_{strakes} = 25\%$

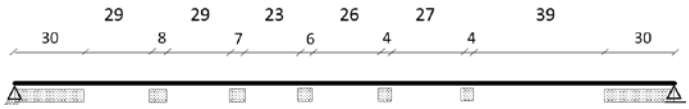

(10) Configuration 10: Multi-span, bare.

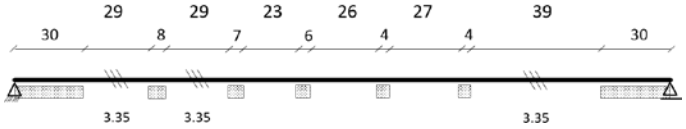

(11) Configuration 11: Multi-span, straked.

Figure 20 Illustration of analysed configurations